Tunneling ionization of vibrationally excited nitrogen molecules

Aleksei S. Kornev* and Boris A. Zon†

Department of Physics, Voronezh State University, 394006 Voronezh, Russia

(Received 22 June 2015; revised manuscript received 14 August 2015; published 21 September 2015)

Ionization of molecular nitrogen plays an important role in the process of light-filament formation in air. In the present paper we theoretically investigated tunneling ionization of the valence $3\sigma_g$ and $1\pi_u$ shells in a N_2 molecule using a strong near-infrared laser field. This research is based on our previously proposed theory of anti-Stokes-enhanced tunneling ionization with quantum accounting for the vibrationally excited states of the molecules [A. S. Kornev and B. A. Zon, Phys. Rev. A **86**, 043401 (2012)]. We demonstrated that if the N_2 molecule is ionized from the ground vibrational state, then the contribution of the $1\pi_u$ orbital is 0.5%. In contrast, for vibrationally excited states with a certain angle between the light polarization vector and the molecule axis, both shells can compete and even reverse their contributions due to the anti-Stokes mechanism. The structure constants of molecular orbitals are extracted from numerical solutions to the Hartree-Fock equations. This approach correctly takes into account the exchange interaction. Quantum consideration of vibrational motion results in the occurrence of the critical vibrational state, the tunneling ionization from which has the maximum rate. The numbers of the critical vibrational states are different for different valence shells. In addition, quantum description of vibrations changes the rate of ionization from the ground vibrational state by 20%–40% in comparison with the quasiclassical results.

DOI: 10.1103/PhysRevA.92.033420 PACS number(s): 33.80.Eh, 33.20.Tp, 42.50.Hz, 33.70.Ca

I. INTRODUCTION

Propagation of an intense laser radiation in the atmosphere accompanied by ionization of atmospheric gases was studied experimentally for the first time in Ref. [1]. Extensive studies in this area are currently being performed (see recent reviews [2,3], papers [4–14], and references therein). To describe theoretically the phenomena emerging in these processes, various models of rovibronic molecular-state populations are introduced [15–17]. Nitrogen is one of the main atmospheric gases. In the present paper we intend to calculate the rate of tunneling ionization of a nitrogen molecule by a laser radiation within a many-body theory. The N_2 molecule is assumed to be in the ground electronic state and in one of its vibrationally excited states. Molecular vibrational excitation before ionization can be caused by the collisions between the molecule and free electrons as well as collisions between the molecule and other atoms and molecules. These collisions occur in the process of filamentation.

The one-body theory of molecule tunneling ionization in an ac field (MO-ADK) was developed in Ref. [18]. The same authors proposed calculating the asymptotic constants of the tunneling electron wave function by the model-potential method [19]. However, the theory from Refs. [18,19] takes into account the nucleus motion only quasiclassically and does not allow for accurate representation of the asymptotic form of the valence electron wave function. Nevertheless, taking into account the vibrational degrees of freedom appears to be rather important. In the tunneling departure of an electron from a molecule, the molecular ion can occur in the ground vibrational state as well as in excited states (see Fig. 1). Since formation of an ion in an excited vibrational state requires higher energy, it is clear that the probability of the ion formation in one of the excited vibrational states is less than that in the ground vibrational state. The appropriate calculations were performed in Ref. [20]. By analogy with the Raman effect, such a decrease in tunneling rate can be called Stokes attenuated. However, if a neutral molecule is initially in an excited vibrational state, then after the tunneling removal of an electron, a molecular ion can occur in the ground vibrational state. Again, with regards to energy, it is clear that the tunneling rate will be greater than that for a neutral molecule in the ground vibrational state. Such an increase in the tunnel-effect rate can be called anti-Stokes enhanced.

In Refs. [21,22], we developed the theory of anti-Stokes-enhanced tunneling ionization of a molecule. Our current work stems from our previous research of studying the many-body effects in the tunneling ionization of atoms [23–29]. The importance of taking into account nuclear motion is demonstrated by the examples of the nonpolar H_2 molecules [21] and the polar hydrogen halide molecules HF and HCl [22] with various isotopic proportions: H, D, ^{18}F, ^{19}F, ^{35}Cl, ^{37}Cl. Particularly, it has been demonstrated that the vibrational excitation of a molecule can significantly increase the tunneling ionization probability (anti-Stokes-enhanced tunnel ionization). Anti-Stokes-enhanced ionization can be used for laser separation of isotopes in addition to the existing methods [30–32]. Our results demonstrate the possibility of obtaining ions with the specified isotopic proportion by selective prepumping of the vibrational states of molecules.

The nitrogen molecule that is under consideration in this research has specific properties which manifest in characteristics of a photoelectron. These properties are caused by the close values of energy of the highest occupied $3\sigma_g$ and $1\pi_u$ orbitals in the ground electronic $X\,^1\Sigma_g^+$ state of the neutral N_2 molecule. The simulations performed by the Hartree-Fock method with the Slater orbitals [33] demonstrate that the energy of the $1\pi_u$ shell lies higher than that of the $3\sigma_g$ shell by 0.5551 eV, whereas the ground state of an N_2^+ ion is $X\,^2\Sigma_g^+$, and the tabulated value of the energy of the first excited electronic state

*a-kornev@yandex.ru
†zon@niif.vsu.ru

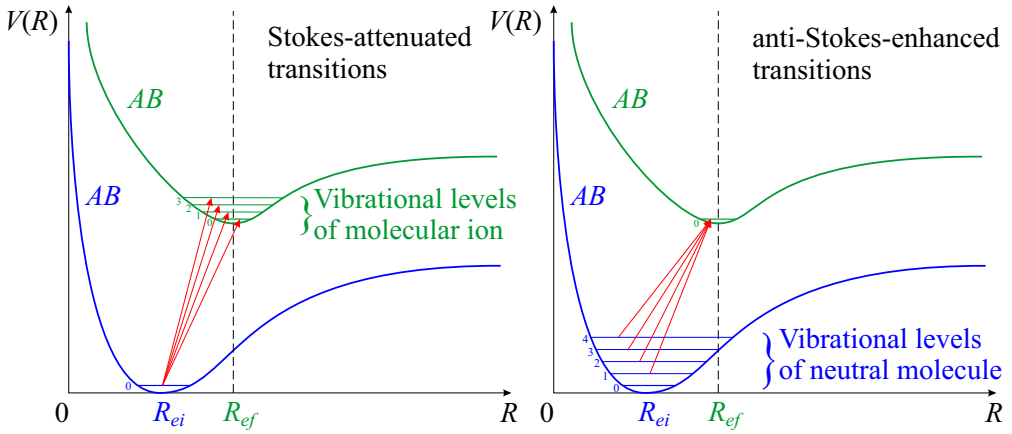

FIG. 1. (Color online) Stokes-attenuated and anti-Stokes-enhanced tunneling transitions in an AB molecule.

$A\,^2\Pi_u$ lies higher by 1.1179 eV [34]. According to the earlier data [35], the ionization potential of the nitrogen molecule from the highest occupied $3\sigma_g$ orbital (HOMO) is equal to 15.6 eV, and that from the $1\pi_u$ orbital (HOMO-1) is equal to 17.2 eV. Thus, in the N_2 molecule, it is necessary to take into account both indicated HOMOs in the calculation of the tunneling ionization rate.

Thus, the motivation of the research can be formulated in three points: (i) application of the previously developed theory to the important practical case of laser filamentation in the air, (ii) accounting for the contribution of two upper shells to the ionization of the nitrogen molecule due to spectral features of the molecule (close values of energies of $3\sigma_g$ and $1\pi_u$ HOMOs), and (iii) improvement of the existing theory [19], particularly, more accurate accounting for structure constants in the nitrogen molecule. In our calculations, the many-body effects are taken into account (Refs. [21,22]), including the possibility of anti-Stokes-enhanced ionization. Accounting for many-body effects shows that the tunneling rate depends not only on the ionization potential of the molecule but also on the equilibrium internuclear separation (through the Franck-Condon factors) and on the frequencies of vibrational transitions (for Stokes-attenuated and anti-Stokes-enhanced processes). Furthermore, a critical value of vibrational quantum number v_c occurs. The tunneling rate from this state has the maximum value. The value of v_c is formed by the competition between the anti-Stokes-enhanced processes and the Franck-Condon factors.

Finally, if not mentioned specifically, the atomic system of units is used throughout.

II. ELECTRON MOTION

In the MO-ADK model [18], the asymptotic form of the valence electron wave function is used at the large distances from the molecular core. In the one-electron approximation for the diatomic homonuclear molecule, this electronic wave function can be written as the spherical harmonic expansion [18],

$$\Psi_m(\mathbf{r}) \approx \mathcal{R}_m(r) \sum_{l=|m|,|m|+2,\ldots}^{\infty} C_l Y_{lm}(\hat{\mathbf{r}}), \qquad \hat{\mathbf{r}} = \mathbf{r}/r, \quad \sum_l |C_l|^2 = 1, \tag{1}$$

where m is conserved projection of the electron angular momentum onto the molecule axis which is assumed to be the quantization axis. $\mathcal{R}_m(r)$ is the asymptotic form of the radial wave function corresponding to the electron binding energy, $\kappa^2/2$,

$$\mathcal{R}_m(r) \approx C\kappa^{3/2}(\kappa r)^{\frac{1}{\kappa}-1}e^{-\kappa r}, \quad r \to \infty. \tag{2}$$

The quantity $\kappa^2/2$ is usually extracted from the experimental data. To calculate κ as well as dimensionless C and C_l constants (so-called structure factors), an approach based on the model-potential method and the density-functional theory was proposed in Refs. [18,19]. The authors of Ref. [18] used the simplest empirical model potential. The authors of Refs. [19,36] obtained one-electron core wave functions with the method of Gaussian orbitals (the GAUSSIAN [37] or GAMESS [38] code). The authors of Ref. [19] constructed the radial parts of the active electron wave function out of the B splines. The motion of the active electrons was considered in the field created by the nuclei and the core electron charge density with the Gaussian asymptotic form. The nonlocal exchange interaction between the tunneling electron and the core was modeled by an additional local term to the potential. The authors of Ref. [36] used specifically improved Gaussian basis functions and direct calculation of the asymptotic form constants without using the model potentials. The significant difference of the Gaussian orbital asymptotic form from the Slater one (2) is the drawback of this method. Therefore, in this research we will use the two-dimensional Hartree-Fock method (x2DHF) developed in Ref. [33] for two atomic molecules. This method provides the correct asymptotic form (2).

First of all, it should be noted that the asymptotic form is valid only at distances so large that the numerical evaluation of the wave function is hard to achieve. To find these constants, it is necessary to obtain such an asymptotic form of the radial wave function that would be valid at moderate distances, where the numerical solution of the Hartree-Fock equations is also possible.

It is convenient to place the origin of coordinates in the middle point between the equilibrium positions of the nuclei. Let the distance between them be equal to R. We expand the wave function of the valence orbital $\Psi_m(R,\mathbf{r})$, found numerically and normalized to unity, over the spherical

TABLE I. Convergence of C values. The first set of values corresponds to the simple comparison of numerical results and Eq. (2). The second set is the result of using Eq. (7).

	$3\sigma_g$		$1\pi_u$	
r (a.u.)	Eq. (2)	Eq. (7)	Eq. (2)	Eq. (7)
10	4.3918	4.2244	2.2882	2.0847
11	4.3973	4.2464	2.2743	2.0891
12	4.4009	4.2636	2.2627	2.0927
13	4.4031	4.2774	2.2527	2.0957
14	4.4045	4.2885	2.2441	2.0982
15	4.4052	4.2976	2.2366	2.1004
16	4.4056	4.3052	2.2299	2.1022
17	4.4056	4.3117	2.2241	2.1038
18	4.4055	4.3172	2.2188	2.1052
19	4.4052	4.3220	2.2141	2.1065
20	4.4049	4.3261	2.2098	2.1075
21	4.4045	4.3297	2.2059	2.1085
22	4.4041	4.3324	2.2024	2.1094
23	4.4037	4.3349	2.1992	2.1102
24	4.4033	4.3373	2.1962	2.1108
25	4.4029	4.3395	2.1934	2.1114
26	4.4025	4.3413	2.1908	2.1119
27	4.4022	4.3428	2.1884	2.1123
28	4.4018	4.3438	2.1862	2.1126
29	4.4016	4.3443	2.1842	2.1129
30	4.4013	4.3445	2.1822	2.1131

functions,

$$\Psi_m(R,\mathbf{r}) = \sum_{l=|m|,|m|+2,\ldots}^{\infty} \tilde{\mathcal{R}}_{lm}(r)\, Y_{lm}(\hat{\mathbf{r}}), \tag{3}$$

where the function

$$\tilde{\mathcal{R}}_{lm}(r) = \int Y^*_{lm}(\hat{\mathbf{r}})\, \Psi_m(R,\mathbf{r})\, d^2\hat{r}$$

is obtained by numerical integration.

At large distances, the radial function $\tilde{\mathcal{R}}_{lm}(r)$ satisfies the radial Schrödinger equation,

$$\Delta_r \tilde{\mathcal{R}}_{lm} + \left[\frac{2}{r} - \kappa^2_{\rm num}\right]\tilde{\mathcal{R}}_{lm} - \frac{l(l+1)}{r^2}\,\tilde{\mathcal{R}}_{lm} = 0, \tag{4}$$

where Δ_r is the radial part of the Laplacian and the value of $\kappa_{\rm num}$ in Eq. (4) is obtained by numerically solving the Hartree-Fock equations.

The asymptotic form of the $\tilde{\mathcal{R}}_{lm}(r)$ function follows from Eq. (4),

$$\tilde{\mathcal{R}}^{\rm (asympt)}_{lm}(r) \approx \kappa^{3/2}_{\rm num}(\kappa_{\rm num} r)^{\nu-1} e^{-\kappa_{\rm num} r} \times \left[1 + \frac{l(l+1) - \nu(\nu-1)}{2\kappa_{\rm num} r} + \ldots\right], \quad r \to \infty, \tag{5}$$

where $\nu = 1/\kappa_{\rm num}$. Unlike Eq. (2), Eq. (5) contains the long-range vanishing term $\sim r^{-1}$. That is why Eq. (5) is more suitable for numerical calculations of C and C_l constants than Eq. (2) since it becomes valid at smaller distances, in contrast to Eq. (2). For $r \to \infty$, the function $\tilde{\mathcal{R}}_{lm}(r)$ turns into $C_l \mathcal{R}_m(r)$ with the substitution $\kappa_{\rm num} \to \kappa$.

The calculation accuracy of $\tilde{\mathcal{R}}_{lm}(r)$ functions can be controlled by means of the quantity

$$c_l = CC_l = \lim_{r\to\infty} \frac{\tilde{\mathcal{R}}_{lm}(r)}{\tilde{\mathcal{R}}^{\rm (asympt)}_{lm}(r)}. \tag{6}$$

Our calculations demonstrate that the stability of result (6) in the third or fourth decimal is achieved at $r > 15$–20 a.u. In turn, neglecting the term $\sim r^{-1}$ in Eq. (5) shifts the stability region up to $r \gtrsim 200$ a.u. Such large distances are often beyond the accuracy of the Hartree-Fock method. For the N_2 molecule, the stability of the constants is improved most noticeably for the $1\pi_u$ orbital (see Table I).

Quantities in Eq. (6) allow us to obtain the C constant:

$$C = \left(\sum_{l=|m|}^{\infty} |c_l|^2\right)^{1/2}. \tag{7}$$

The values of C and C_l for the $3\sigma_g$ and $1\pi_u$ orbitals of the N_2 molecule are given in Table II and are compared with the results obtained with the model-potential methods (Refs. [18,19]). One can see that our results differ from those obtained in Ref. [19] mainly in the magnitude of the C constant. This can originate from a more accurate accounting of the exchange interaction, without the use of a model potential.

The method to calculate the structure constants presented here is analogous to that proposed in Ref. [36], where an improved Gaussian basis set was used. As a result, at moderate distances, the form of the wave function is close to the Slater one, whereas at large distances, it becomes Gaussian. The method from Ref. [36] is convenient for investigating polyatomic molecules, where directly solving the Hartree-Fock equations is technically difficult.

TABLE II. Values of C and C_l constants obtained from Eqs. (6) and (7) for the valence $3\sigma_g$ and $1\pi_u$ shells in the N_2 molecule. Corresponding results from Refs. [18,19] are scaled to dimensionless units and given here for comparison.

Shell	C	$C_{\lvert m\rvert}$	$C_{\lvert m\rvert+2}$	$C_{\lvert m\rvert+4}$	$C_{\lvert m\rvert+6}$	Source
$3\sigma_g$ ($\lvert m\rvert = 0$,	1.9159	0.9327	0.3602	0.0185		[18]
$\kappa_{\rm num} = 1.1265$ a.u.)	2.5634	0.9249	0.3796	0.0207		[19]
	4.3445	0.9427	0.3333	0.0132	0.0002	this work
$1\pi_u$ ($\lvert m\rvert = 1$,	1.5788	0.9933	0.1156	0.0053		[19]
$\kappa_{\rm num} = 1.1082$ a.u.)	2.1130	0.9972	0.0750	0.0015		this work

III. DYSON ORBITAL

The Born-Oppenheimer approximation (BOA) is commonly used in studies of interactions between molecules and electromagnetic radiation. However, dissociative ionization and Coulomb explosion are exceptional cases for which BOA does not apply (e.g., [39–43]). This case is not considered in the present work. In the process of tunnel ionization of molecules, nonadiabatic retardation effects can arise, leading to breaking the validity of the BOA. These effects were examined for a hydrogen molecule in [44]. They become apparent in changing the electron density at large distances from the molecule. In accordance with [44], if the reduced mass of the nuclei of a hypothetical hydrogen molecule is 125 times higher than the electron mass, the electron density deviates from the BOA predictions by more than 10% at distances greater than 10 a.u. If the excess is more than 500 times, the BOA will be valid up to distances of 15–20 a.u. The constants in Eq. (6) are calculated at such distances. These quantities are necessary for obtaining the asymptotic form (2). In ordinary molecules, the reduced mass of nuclei exceeds the electron mass by more than ∼2000 times, making the BOA valid for distances exceeding 25 a.u. Therefore, there is no need to go beyond the BOA.

For a complete description of the molecule's stationary states in the framework of the BOA, many-electron functions must be multiplied by the nuclei vibrational motion wave functions,

$$\Psi_{\mu,v_\mu}(\mathbf{R},\{\mathbf{r}\}) = \chi_{\mu,v_\mu}(\mathbf{R})\,\Phi_\mu(\mathbf{R},\{\mathbf{r}\}), \quad \mu = i,f, \tag{8}$$

where $\{\mathbf{r}\}$ is the set of electron coordinates, Φ_μ is the many-electron wave function taken at the fixed equilibrium internuclear separation R, the χ_{μ,v_μ} function describes the vibrational stationary state with the quantum number $v_\mu = 0,1,\ldots$, and the $\mathbf{R}$ vector specifies the molecule orientation. The μ index marks the state of the molecule.

In the traditional ADK and MO-ADK models, the atomic or ionic core is considered to be "frozen," meaning its states do not change after tunneling electron departure. However, the electron wave functions of core electrons in a neutral molecule and in a molecular ion generally differ. The Dyson orbital, presenting integral overlap between the electron configurations of a neutral molecule in the initial state ($\mu = i$) and its ion in the final state ($\mu = f$), should be used to take into account the differences between the core electron functions. According to Eq. (8),

$$\Psi^{(\mathrm{Dyson})}_{v_f\,v_i}(\mathbf{r}) = \int_0^\infty \chi^*_{f,v_f}(R)\chi_{i,v_i}(R)\,dR \times \int \Phi^*_f(R,\{\mathbf{r}'\})\,\Phi_i(R;\mathbf{r},\{\mathbf{r}'\})\,\{d^3r'\}, \tag{9}$$

where $\mathbf{r}$ is the coordinate of an active valence electron and $\{\mathbf{r}'\}$ is the set of core electron coordinates. The significance of using the Dyson orbital in studying molecule ionization was demonstrated in Refs. [45–48].

Collisionless orientation of the molecule's axes along the direction of the light-wave electric vector occurs in strong laser fields [49–53]. In Ref. [54], direct observation was carried out for the influence of molecule orientation upon ionization. In the present work, we do not take into account this effect, considering ionizing laser pulses to be sufficiently short. For long pulses, accounting for orientation is not difficult. Thus, the notation R is used in Eq. (9) instead of $\mathbf{R}$.

Equation (9) can be simplified by taking into account the small amplitude of classical vibrations compared to the equilibrium internuclear separation $R_{ei,f}$ and the Hartree-Fock approximation (see details in Ref. [21]),

$$\Psi^{(\mathrm{Dyson})}_{v_f\,v_i}(\mathbf{r}) \approx I^{(v)}_{fi} I^{(e)}_{fi} \Psi_m(R_{ei},\mathbf{r}). \tag{10}$$

Here, $\Psi_m(R_{ei},\mathbf{r})$ corresponds to the one-body state of the active electron with the momentum projection on the molecule axis equal to m (for a σ orbital, $m = 0$ and for a π orbital, $m = \pm 1$). The asymptotic form of Ψ_m is given by Eqs. (1) and (2). The calculation algorithm for the structure factors C and C_l is described in the previous section. $I^{(e)}_{fi}$ is the overlap integral between the core electronic states in the neutral molecule and in its ion. It can be found analytically in terms of the parameters produced by the GAUSSIAN code (see the Appendix). To calculate $I^{(e)}_{fi}$ in same molecules but with different isotopic proportions, the origin of the coordinates is placed in the center of mass of the nuclei. In our case using the $^{14}N_2$ molecule,

$$I^{(e)}_{fi}\left[\mathrm{N_2}\left(X\,^1\Sigma^+_g\right) \to \mathrm{N_2^+}\left(X\,^2\Sigma^+_g\right)\right] = 0.9797,$$
$$I^{(e)}_{fi}\left[\mathrm{N_2}\left(X\,^1\Sigma^+_g\right) \to \mathrm{N_2^+}\left(A\,^2\Pi_u\right)\right] = 1.0102.$$

These data are obtained by using the augmented correlation-consistent polarized valence five zeta (AUG-cc-pV5Z) basis set.

$$I^{(v)}_{fi} = \int_0^\infty \chi^*_{f,v_f}(R)\chi_{i,v_i}(R)\,dR \tag{11}$$

is the overlap integral between vibrational states. Its square is the Franck-Condon factor. The next section deals with the calculation of the $I^{(v)}_{fi}$ integral. Each factor in Eq. (10) depends on $R_{ei,f}$ parametrically.

IV. ACCOUNTING FOR VIBRATIONAL MOTION

The vibrational motion in molecules is conveniently modeled by the Morse potential. The energy spectrum of this motion has the form

$$E_v = \omega_e\left(v+\tfrac{1}{2}\right) - x_e\omega_e\left(v+\tfrac{1}{2}\right)^2, \quad v = 0,1,\ldots, \tag{12}$$

where v is the vibrational quantum number, ω_e is the vibration frequency, and x_e is the first anharmonicity constant. The parameters of spectrum (12) for the $^{14}N_2$ molecule and its positive ion are taken from Ref. [34] and given in Table III.

TABLE III. Values of parameters of the N_2 molecule and of its positive ion. Here, Δ is the energy of the electron excitation, R_e is the equilibrium internuclear separation, ω_e is the vibration frequency for the molecule consisting of the ^{14}N isotope, and x_e is the first anharmonicity constant. The data are taken from Ref. [34].

Molecule	Δ (cm^{-1})	R_e (Å)	ω_e (cm^{-1})	$x_e\omega_e$ (cm^{-1})
$N_2(X\,^1\Sigma^+_g)$	0	1.098	2359	14.3
$N_2^+(X\,^2\Sigma^+_g)$	0	1.116	2207	16.1
$N_2^+(A\,^2\Pi_u)$	9016.4	1.174	1903	14.9

TABLE IV. Values of dynamic molecular polarizabilities and of their derivatives (in atomic units) in the case of equilibrium internuclear separation in the N_2 molecule and in its ions (see Table III). The Gaussian AUG-cc-pV5Z basis set was used in the calculations. The radiation frequency corresponds to the wavelength of the Ti:sapphire near-infrared laser radiation of 800 nm. Numerical differentiation was performed within five points in steps of 0.005 Å.

Molecule	$\alpha_\parallel$	$\alpha_\parallel^{(1)}$	$\alpha_\parallel^{(2)}$	$\alpha_\perp$	$\alpha_\perp^{(1)}$	$\alpha_\perp^{(2)}$
$N_2(X\,^1\Sigma_g^+)$	15.8369	15.0926	10.0856	10.3834	5.6866	3.6514
$N_2^+(X\,^2\Sigma_g^+)$	9.2132	17.7573	−3.0724	6.6153	3.1883	−0.5720
$N_2^+(A\,^2\Pi_u)$	11.1186	18.0953	1.1358	6.9600	3.1395	0.0198

The value of integral (11) can be found numerically with the vibrational functions for the Morse potential. The value of (11) is determined by the equilibrium internuclear separations $R_{ei,f}$, by the vibrational frequencies $\omega_{ei,f}$, by the first anharmonicity constants $x_{ei,f}$, and by the vibrational quantum numbers $v_{i,f}$ in the neutral molecule and its ion, respectively (see also Ref. [22]).

An external laser field modifies the parameters of the molecule vibrations. This effect was taken into account in Ref. [55] in the Born-Oppenheimer approximation in the field of monochromatic linearly polarized laser radiation. The response of the molecular vibrations to the external field is determined by the tensor of dynamic molecular polarizability $\alpha_{ij}(\omega,R)$, depending on the internuclear separation R and on the frequency of external field ω (Table IV). For a nonrotating molecule, the change in energy in the external monochromatic field (the quadratic dynamic Stark effect) is given by the expression

$$\Delta E(\omega,\mathbf{R}) = -\tfrac{1}{4}\,\alpha(\omega,\mathbf{R})F^2.$$

Hereinafter, F is laser field strength amplitude,

$$\alpha(\omega,\mathbf{R}) = \alpha_\parallel(\omega,R)\cos^2\theta + \alpha_\perp(\omega,R)\sin^2\theta, \tag{13}$$

$\alpha_\parallel$ and $\alpha_\perp$ are longitudinal and transversal components of the tensor of dynamic polarizability with respect to the molecule axis, respectively, and θ is the angle between the molecule axis and the vector of radiation polarization.

In Ref. [55], it was demonstrated that the polarizing influence of the laser field on the molecule leads to the change in the molecule vibrational parameters. In the adiabatic approximation, when the nuclei vibration cycle is significantly shorter than the time required to change the laser radiation intensity, the vibrational parameters are modified according to the formulas

$$R_e = R_e^{(0)}\left[1 + \frac{\alpha^{(1)}F^2}{4M\omega_e^2 R_e^{(0)}}\right], \tag{14}$$

$$\omega_e = \left[\omega_e^{(0)2} - \frac{\alpha^{(2)}F^2}{4M}\right]^{1/2}. \tag{15}$$

Here,

$$\alpha^{(\nu)} = \left.\frac{\partial^\nu \alpha}{\partial R^\nu}\right|_{R=R_e^{(0)}}, \quad \nu = 1,2,$$

and M is the reduced mass of the nuclei. The superscript (0) corresponds to the frequency ω_e and the separation R_e in the absence of external fields. From Eqs. (14) and (15) one can see that in the external field, the parameters of vibrations are determined not only by intensity but by the isotopic proportion in the molecules. As we demonstrated in Ref. [21] for the example of a hydrogen molecule, accounting for the laser field's influence upon the molecule vibrations can lead to the double change of the molecular ion yield.

The tensor components $\alpha_{ij}(\omega,R)$ can be obtained, for example, within the method of Gaussian orbitals. In this study, calculations were performed with the DALTON code [56,57], which allows us to implement the calculation algorithm in the multiconfigurational approximation. The interaction between all electron orbitals was taken into account (complete active space). The AUG-cc-pV5Z Gaussian basis set was used.

V. TUNNELING RATE

In the linearly polarized monochromatic laser field $\mathbf{F}_0\cos\omega t$, the cycle-averaged tunneling rate is given by the formula from Refs. [18,21,22],

$$W_{fi}(F_0,\mathbf{R}_{ei}) = C^2\kappa_{fi}^2 I_{fi}^{(e)2} I_{fi}^{(v)2} \sum_{m'} \frac{B_{m'}^2(\mathbf{R}_{ei})}{2^{|m'|}|m'|!}\sqrt{\frac{3F_0}{\pi\kappa_{fi}^3}} \times \left(\frac{2\kappa_{fi}^3}{F_0}\right)^{2\nu_{fi}-|m'|-1} \exp\left[-\frac{2\kappa_{fi}^3}{3F_0}\right]. \tag{16}$$

Here,

$$B_{m'}(\mathbf{R}_{ei}) = (-1)^{m'}\sum_l C_l D_{m',m}^l(\mathbf{R}_{ei})\sqrt{\frac{2l+1}{2}\frac{(l+|m'|)!}{(l-|m'|)!}}.$$

The constants C and C_l determine the asymptotic form of the valence one-electron orbitals (1) and (2), and m is the tunneling electron orbital momentum projection onto the molecule axis. The quantization axis (z) of the laboratory frame is directed along $\mathbf{F}_0$. The standard notation for the Wigner D function is introduced.

The parameter κ_{fi} in the inelastic tunnel effect theory [20,23–29] is determined by the experimental ionization potential of the molecule $I_{\rm exp}$, by the excitation energies, and by the quadratic Stark effect [29],

$$\kappa_{fi} = \sqrt{2}\big[I_{\rm exp} + E_{v_f}^{(f)} - E_0^{(f)} + E_0^{(i)} - E_{v_i}^{(i)} + \Delta + \Delta_{\rm Stark}(\omega;\mathbf{R}_{ef},\mathbf{R}_{ei};\mathbf{F}_0)\big]^{1/2}, \tag{17}$$

where $E_{v_{i,f}}^{(i,f)}$ are the vibrational energy levels in the neutral molecule (i) and its ion (f), respectively, Δ is the electron excitation energy in the ion (see Table III), and the quantity

$$\Delta_{\rm Stark}(\omega;\mathbf{R}_{ef},\mathbf{R}_{ei};\mathbf{F}_0) = \tfrac{1}{4}[\alpha_i(\omega,\mathbf{R}_{ei}) - \alpha_f(\omega,\mathbf{R}_{ef})]F_0^2$$

is determined by the Stark shift of energies in the neutral molecule and in its ion. As before, values of $\alpha_{i,f}$ are determined by Eq. (13).

Results from Ref. [21] demonstrate that $\kappa_{\rm num}$ differs from κ_{fi} not more than by 5%. Two causes can be proposed to explain the given difference: (i) neglecting the residual interaction within the Hartree-Fock method and (ii) neglecting the nuclear vibrations when we simulate the one-electron wave

functions. The quantity $\kappa_{\rm num}^2/2$ is also referred to as the vertical ionization potential. Therefore, we use the experimental values of κ_{fi} in Eq. (16), as required by the ADK model, while to obtain the C and C_l coefficients, we use the calculated value of $\kappa_{\rm num}$. Using $\kappa_{\rm num}$ instead of κ_{fi} is required here only to ensure self-consistency of the calculation algorithm. We introduced the notation $\nu_{fi} = \kappa_{fi}^{-1}$ in Eq. (16).

Our modification of the MO-ADK theory is in quantum, not quasiclassical [18], consideration of molecular vibrations. It manifests specifically not only in changing κ through the ionization potential but also in the appearance of the Franck-Condon factors as well as in accounting for Stokes-attenuated and anti-Stokes-enhanced transitions.

In the case of the linear molecule, the ionization rate is dependent on the azimuthal angle θ_e. Let us consider the molecule preexcited to the v_ith vibrational state. Then, with the given ionization intensity, the ionization rate will be a function of the angle θ_e between the molecule axis and the vector of radiation polarization. Quantity (16) is to be summed up over all possible vibrational states of the molecular ion,

$$W_{v_i}(F_0,\theta_e) = \sum_{v_f} W_{fi}(F_0,\mathbf{R}_e). \tag{18}$$

VI. NUMERICAL RESULTS AND DISCUSSION

We examined the $^{14}N_2$ molecule ionization in two ways: by removing an electron from the $3\sigma_g$ and $1\pi_u$ orbitals. The experimental value of its ionization potential, $I_{\rm exp} =$ 15.580 eV [34], is close to that of the HF molecule (15.77 eV). As it was calculated for the HF molecule placed in the focal volume of the laser beam with the Gaussian envelope over both time and the beam diameter and with a pulse FWHM of 100 fs [22], the ionization signal becomes saturated if the peak intensity in the focus is higher than 10^{14} W/cm^2.

As obtained previously in Refs. [21,22], in the saturation region, the anti-Stokes-enhanced effects become weaker as the intensity increases. Therefore, at first, we will perform an investigation for a fixed value of intensity of 3.5×10^{13} W/cm^2. Thus, for the N_2 molecule, according to Eq. (18), we calculated the tunneling ionization rate as a function of the angle θ_e with the intensity value mentioned above and various values of v_i. The results for ionization of the $3\sigma_g$ and $1\pi_u$ shells by the monochromatic radiation are given in Figs. 2–4.

It is interesting to compare the different results obtained with the different values of the structure factors. Particularly, the first set of structure factors was obtained in Ref. [19], and we calculated the second one in the present paper using the x2DHF method [33] (see Table II). For comparison with the results of the "pure" MO-ADK model, we restrict ourselves to the tunneling transitions between the ground vibrational states. The ionization rate for the $3\sigma_g$ shell of an N_2 molecule as a function of the angle θ_e between the molecule axis and an electric field vector is given in Fig. 2. One can see that, according to the data from Table II, correctly accounting for the exchange interaction within the x2DHF method causes the ionization rate of the $3\sigma_g$ orbital to triple and that of the $1\pi_u$ orbital to double. This disagreement is caused by the change in the structure constant C. We also note the decrease in the rate of tunneling ionization from the ground vibrational state

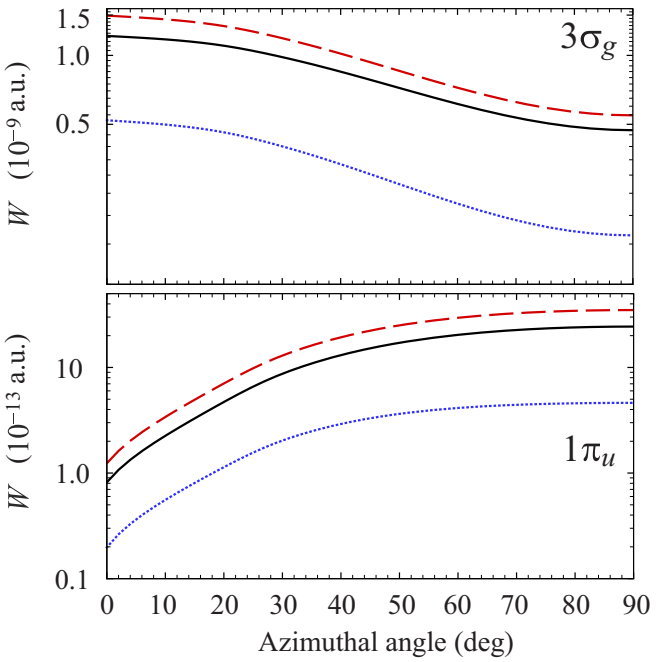

FIG. 2. (Color online) Ionization rate for the $3\sigma_g$ and $1\pi_u$ shells of an N_2 molecule as a function of an angle, θ_e, between the molecule axis and an electric field vector. The intensity of the linearly polarized monochromatic radiation is fixed and equal to 3.5×10^{13} W/cm^2. Solid lines: our results while accounting for molecular vibrations for $v_i = 0$. Dashed lines: results obtained with our values of molecular parameters but neglecting molecular vibrations. Dotted lines: results obtained with the parameters from Ref. [19] and with the ionization potentials from Ref. [35] (the "pure" MO-ADK theory).

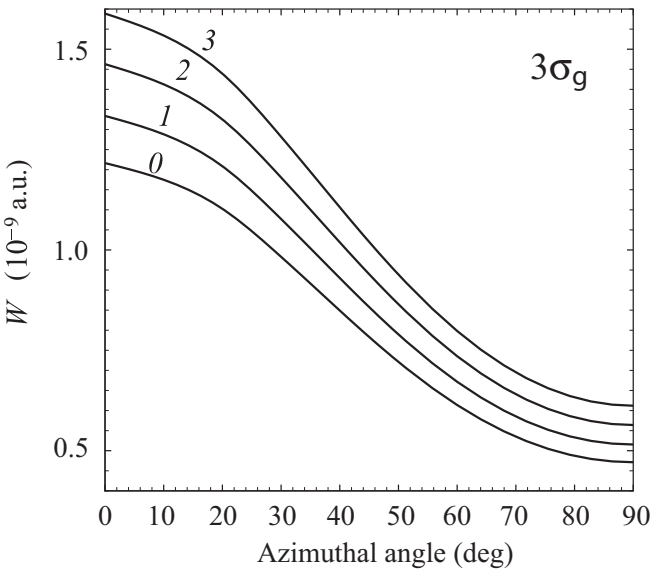

FIG. 3. Ionization rate for the $3\sigma_g$ shell of an N_2 molecule as a function of an angle, θ_e, between the molecule axis and an electric field vector. The intensity of the linearly polarized monochromatic radiation is fixed and equal to 3.5×10^{13} W/cm^2. The values of the vibrational quantum number of neutral molecules v_i are indicated.

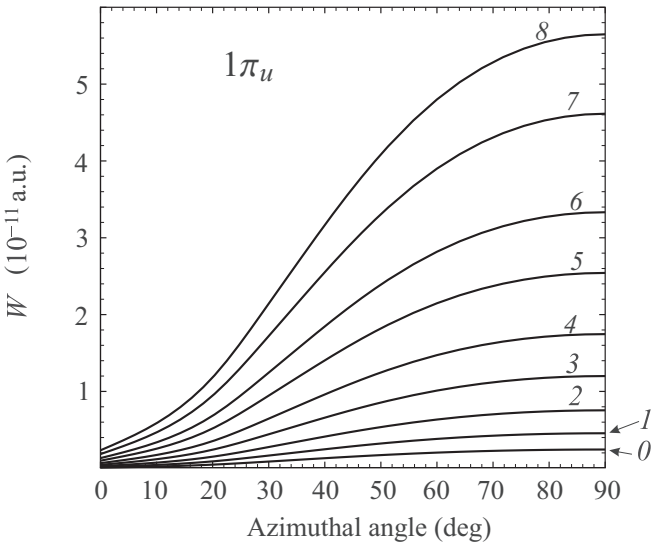

FIG. 4. Same as in Fig. 3 but for the $1\pi_u$ shell.

of a neutral molecule ($v_i = 0$) by 20%–40% in the case of quantum accounting for vibrations. This effect occurs due to the Franck-Condon factors. Their absolute values are less than unity.

Ionization suppression for the $1\pi_u$ shell in the case when the molecule is oriented along the polarization vector (see Figs. 2 and 4) is easy to explain within the framework of the tunneling theory. The process is most probable for states with the zero projection of the electron orbital momentum m' onto the direction of the electric vector of the laser radiation. If $m' \neq 0$, then the process is suppressed. But in the states with $m' \neq 0$, the contribution of projection $m = 0$ onto the direction perpendicular to the molecule axis will be nonzero according to the general theory of the angular momentum. Therefore, ionization of π shells is most efficient at the mutually orthogonal orientation of the molecule axis and radiation polarization vector. Hence, the significant qualitative difference between the ionizations of $3\sigma_g$ and $1\pi_u$ shells appears.

Figures 3 and 4 also demonstrate the anti-Stokes-enhanced ionization of the excited vibrational states of a neutral molecule. This effect is better seen for the $1\pi_u$ shell. Possibly, this effect can be attributed to the more significant difference between the frequencies of N_2 and $N_2^+(A\,^2\Pi_u)$ than between those of N_2 and $N_2^+(X\,^2\Sigma_g^+)$ (see Table III) since the κ_{fi} parameter in (17) depends on these frequencies and the tunneling exponential factor in Eq. (16) depends on κ_{fi}.

In Ref. [19], ionization of HOMO-2 was also considered. This orbital has a one-electron configuration with $2\sigma_u$ symmetry and an ionization potential of 18.7 eV [35]. It lies immediately below HOMO-1. As one can see from Fig. 3(a) in Ref. [19], for a small orientation angle θ_e with respect to the polarization vector, the contribution of the deeper $2\sigma_u$ shell exceeds the contribution of the $1\pi_u$ shell due to the above-mentioned features of their symmetries. Both shells start to compete as θ_e increases. For an intensity of 1.5×10^{14} W/cm^2, the contributions of the shells reverse if $\theta_e > 35^\circ$. However, within the framework of the "pure" MO-ADK theory, the $3\sigma_g$ (HOMO) and $1\pi_u$ (HOMO-1) orbitals do not compete.

TABLE V. Values of $W_{v_i}(1\pi_u)/W_{v_i}(3\sigma_g)$ for an N_2 molecule orientated perpendicular to the laser radiation polarization vector ($\theta_e = 90^\circ$). The radiation intensity is 3.5×10^{13} W/cm^2.

v_i	$W_{v_i}(1\pi_u)/W_{v_i}(3\sigma_g)$	v_i	$W_{v_i}(1\pi_u)/W_{v_i}(3\sigma_g)$
0	5.175×10^{-3}	5	5.640×10^{-2}
1	8.840×10^{-3}	6	0.3170
2	1.337×10^{-2}	7	4.265
3	1.961×10^{-2}	8	104.1
4	2.984×10^{-2}	9	3157

An interesting result of our research is the possible competition between the $3\sigma_g$ and $1\pi_u$ shells in the case of ionization from highly excited vibrational states of the neutral N_2 molecule which is oriented perpendicular to the radiation polarization vector. The ratio of the ionization rate from the $1\pi_u$ shell to that from the $3\sigma_g$ shell is given in Table V as a function of the vibrational quantum number v_i in the neutral N_2 molecule. For the ground vibrational state of N_2, the ionization rate for the $3\sigma_g$ shell is higher than that for the $1\pi_u$ shell by 200 times. In contrast, for the excited state with $v_i = 6$, the contribution of the $1\pi_u$ shell exceeds 30%, and in the excited state with $v_i = 9$, the ionization rate for the $1\pi_u$ shell is higher than that for the $3\sigma_g$ shell by ~3000 times. The competition occurs in spite of the double excess of the structure factor C in the $3\sigma_g$ shell and electron excitation in the $N_2^+(A\,^2\Pi_u)$ ion.

Nevertheless, it should be noted that the possibility of the anti-Stokes-enhanced tunneling ionization is limited to the critical value of the vibrational quantum number v_c. Particularly, for the $3\sigma_g$ shell of N_2, $v_c = 3$, and for the $1\pi_u$ shell, $v_c = 8$ (see also Table VII below). With higher values of v (for the N_2 molecule within the framework of the Morse potential model $v \leqslant 82$) the anti-Stokes enhancement effect does not occur due to the decrease of the Franck-Condon factors (see Table VI).

Thus, due to the presence of the anti-Stokes channels, the competition between the $3\sigma_g$ and $1\pi_u$ shells of the N_2 molecule oriented perpendicular to the laser electric field vector is possible.

TABLE VI. Values of the Franck-Condon factors, $f_{v_i}^{(1)} = I_{fi}^{(v)2}[N_2, v_i \to N_2^+(X\,^2\Sigma_g^+), v_f = 0]$ and $f_{v_i}^{(2)} = I_{fi}^{(v)2}[N_2, v_i \to N_2^+(A\,^2\Pi_u), v_f = 0]$, for ionization transitions in the N_2 molecule.

v_i	$f_{v_i}^{(1)}$	$f_{v_i}^{(2)}$
0	9.269×10^{-1}	2.764×10^{-1}
1	7.102×10^{-2}	3.812×10^{-1}
2	2.055×10^{-3}	2.340×10^{-1}
3	3.557×10^{-5}	8.459×10^{-2}
4	3.438×10^{-7}	2.009×10^{-2}
5	2.099×10^{-9}	3.309×10^{-3}
6	8.314×10^{-12}	3.893×10^{-4}
7	5.922×10^{-16}	3.319×10^{-5}
8	1.099×10^{-15}	2.060×10^{-6}
9	1.418×10^{-15}	9.270×10^{-8}

TABLE VII. Values of Eq. (19) (in atomic units) as functions of intensity and v_i for ionization transitions in the N_2 molecule.

	0.5×10^{14} W/cm^2		1.0×10^{14} W/cm^2		1.5×10^{14} W/cm^2	
v_i	$3\sigma_g$	$1\pi_u$	$3\sigma_g$	$1\pi_u$	$3\sigma_g$	$1\pi_u$
0	4.190×10^{-8}	1.878×10^{-10}	2.009×10^{-5}	2.106×10^{-7}	2.992×10^{-4}	4.641×10^{-6}
1	4.496×10^{-8}	3.033×10^{-10}	2.099×10^{-5}	2.732×10^{-7}	3.095×10^{-4}	5.484×10^{-6}
2	4.827×10^{-8}	4.499×10^{-10}	2.194×10^{-5}	3.385×10^{-7}	3.200×10^{-4}	6.244×10^{-6}
3	5.124×10^{-8}	6.650×10^{-10}	2.254×10^{-5}	4.483×10^{-7}	3.240×10^{-4}	7.897×10^{-6}
4	4.684×10^{-8}	8.940×10^{-10}	1.918×10^{-5}	5.302×10^{-7}	2.665×10^{-4}	8.792×10^{-6}
5	3.476×10^{-8}	1.229×10^{-9}	1.307×10^{-5}	6.684×10^{-7}	1.754×10^{-4}	1.068×10^{-5}
6	7.446×10^{-9}	1.500×10^{-9}	2.396×10^{-6}	7.263×10^{-7}	2.999×10^{-5}	1.097×10^{-5}
7	6.922×10^{-10}	1.975×10^{-9}	1.877×10^{-7}	8.852×10^{-7}	2.164×10^{-6}	1.293×10^{-5}
8	3.145×10^{-11}	2.291×10^{-9}	7.204×10^{-9}	9.402×10^{-7}	7.663×10^{-8}	1.324×10^{-5}
9	7.555×10^{-13}	1.746×10^{-9}	1.440×10^{-10}	6.346×10^{-7}	1.392×10^{-9}	8.508×10^{-6}

For randomly oriented diatomic molecules, it is necessary to average quantity (18) over the directions of the $\mathbf{R}_e$ vector. In the case of a symmetrical molecule (e.g., N_2), this averaging can be performed by the simple integration

$$\tilde{W}_{v_i}(F_0) = \int_0^{\pi/2} W_{v_i}(F_0,\theta_e) \sin\theta_e \, d\theta_e. \tag{19}$$

In Table VII, the values of $\tilde{W}$ are given for several values of intensity and v_i. One can see that the main regularities from Table V are valid for higher intensities. However, in the saturation region, the anti-Stokes-enhanced effects appear to be weaker, in accordance with the results from Refs. [21,22]. For an intensity of 1.5×10^{14} W/cm^2 and $v_i = 0$, the relative difference between our results and those in Ref. [19] agrees with the data from Fig. 2. Indeed, for the ground vibrational state of the neutral molecule ($v_i = 0$), our theory differs from Ref. [19] mainly in the preexponential factor.

The results given in Table VII are important for the research of filamentation because they are the rate constants for elementary processes in a plasma. They are necessary for the description of filamentation kinetics (spark evolution).

VII. CONCLUSION

Calculations of the tunneling ionization rate performed for the nitrogen molecule demonstrate that the structure constant of molecular orbitals is very sensitive to the method of the wave-function simulation. Correctly accounting for the exchange interaction in the course of solving the Hartree-Fock equations results in a significant change in the structure constants in molecular orbitals compared to the model-potential methods. As a result, the rate of tunneling ionization of the molecule can be increased by 2 to 3 times.

Quantum accounting for vibrational motion results in a change in the ionization rate by 20%–40% for the transition between the ground vibrational states of the neutral nitrogen molecule and its ion. Such a difference is caused by the values of the Franck-Condon factors for these states. Combined accounting for the anti-Stokes-enhanced transitions and the quantum effects in the molecular vibrations leads to the occurrence of the critical vibrational quantum number of a neutral molecule v_c. The tunneling rate has the maximum value in the state with this value of the vibrational quantum number.

Excitation of vibrational states of a nitrogen molecule significantly changes the rate of its tunneling ionization. Ionization of the $3\sigma_g$ orbital from the ground vibrational state of a nitrogen molecule will occur with a higher probability than that of the $1\pi_u$ orbital due to the specifics of the electron structure, despite the close values of energy of both orbitals. However, the preexcitation of vibrations in a neutral $^{14}N_2$ molecule leads to the increase in the contribution of the $1\pi_u$ orbital in the anti-Stokes ionization channel. If the value of the vibrational quantum number exceeds 6, the contribution of the $1\pi_u$ orbital becomes dominant.

ACKNOWLEDGMENTS

This research was carried out under financial support of the Ministry of Education and Science of the Russian Federation (State Order No. 3.1306.2014/K). The authors thank Dr. A. Jaroń-Becker for interest in the research.

APPENDIX

To calculate the overlap electron integrals $I_{fi}^{(e)}$ in Eq. (10), it is convenient to expand an electron orbital of the core ψ_e over the linear combinations of the primitive Gaussians,

$$\psi_e(\mathbf{r}) = \sum_{ij} c_{ij} g_{ij}(\mathbf{r} - \mathbf{R}_i). \tag{A1}$$

Here, $\mathbf{R}_i$ is the equilibrium position of the ith nucleus in the center-of-mass system, c_{ij} are coefficients calculated with the GAUSSIAN code, and

$$g_{ij}(\mathbf{r}) = x^{n_{xij}} y^{n_{yij}} z^{n_{zij}} \exp[-\xi_{ij}(x^2 + y^2 + z^2)] \tag{A2}$$

is the primitive Gaussian in Cartesian coordinates. Its parameters, n_{xij}, n_{yij}, n_{zij}, and ξ_{ij}, are determined by the basis set.

The orbitals in a neutral molecule, $\psi_{ei}(\mathbf{r})$, and in its ion in the ground electronic state, $\psi_{ef}(\mathbf{r})$, differ only in the coefficients c_{ij} and in the positions of the nuclei $\mathbf{R}_i$. Therefore, it is sufficient to obtain the expression for the overlap integral between two primitive Gaussians which are centered on different nuclei of the neutral molecule and its ion.

The primitive Gaussian (A2) has an important property: the product of two given primitive Gaussians is the finite linear combination of other Gaussians. They have the same exponents ξ and coordinates of the common center $\mathbf{R}$ but

different power exponents of coordinates, n_{xij}, n_{yij}, and n_{zij}. This statement follows from the properties of the Gaussian exponent and binomial expansion. Particularly,

$$\exp[-\xi_1(\mathbf{r}-\mathbf{R}_1)^2]\exp[-\xi_2(\mathbf{r}-\mathbf{R}_2)^2] = \exp[-\xi(\mathbf{R}_1-\mathbf{R}_2)^2]\exp[-\Xi(\mathbf{r}-\mathbf{R})^2], \tag{A3}$$

where

$$\Xi = \xi_1+\xi_2, \quad \xi = \xi_1\xi_2/\Xi, \quad \mathbf{R} = (\xi_1\mathbf{R}_1+\xi_2\mathbf{R}_2)/\Xi.$$

In view of the above, we obtain the following analytical expression for the overlap integral between two primitive Gaussians:

$$\int g_{i'j'}(\mathbf{r}-\mathbf{R}_{i'})g_{ij}(\mathbf{r}-\mathbf{R}_i)\,d^3r$$
$$= \left(\frac{\pi}{\Xi}\right)^{3/2}\exp(-\Xi R^2)S(\Xi;X_1,n_{xi'j'};X_2,n_{xij})S(\Xi;Y_1,n_{yi'j'};Y_2,n_{yij})S(\Xi;Z_1,n_{zi'j'};Z_2,n_{zij}). \tag{A4}$$

Here,

$$\Xi = \xi_{i'j'}+\xi_{ij},\ \xi = \xi_{i'j'}\xi_{ij}/\Xi,\ \mathbf{R} = (\xi_{i'j'}\mathbf{R}_{i'}+\xi_{ij}\mathbf{R}_i)/\Xi,$$
$$\{X_1,Y_1,Z_1\} = \mathbf{R}\xi_{ij}/\Xi, \quad \{X_2,Y_2,Z_2\} = -\mathbf{R}\xi_{i'j'}/\Xi, \tag{A5}$$
$$S(\Xi;V_1,l_1;V_2,l_2) = \sum_{n_1,n_2=0,1,\ldots}(q-1)!!\binom{l_1}{n_1}\binom{l_2}{n_2}\frac{V_1^{n_1}V_2^{n_2}}{(2\Xi)^{q/2}}.$$

In Eq. (A5), the summation involves only even non-negative values of

$$q = l_1+l_2-n_1-n_2.$$

The standard notation for the binomial coefficient is introduced in Eq. (A5). Formula (A4) was derived by using the Poisson integral,

$$\int_{-\infty}^{+\infty}x^{2k}e^{-x^2}dx = (2k-1)!!\sqrt{\pi}/2^k, \quad k = 0,1,\ldots$$

The analytical form of the overlap integral $I_{fi}^{(e)}$ is a finite linear combination of integrals (A4) with the coefficients $c_{i'j'}c_{ij}$. It is not given here.

[1] A. Brodeur, C. Y. Chien, F. A. Ilkov, S. L. Chin, O. G. Kosareva, and V. P. Kandidov, Moving focus in the propagation of ultrashort laser pulses in air, Opt. Lett. **22**, 304 (1997).

[2] S. V. Chekalin and V. P. Kandidov, From self-focusing light beams to femtosecond laser pulse filamentation, Phys. Usp. **56**, 123 (2013).

[3] A. A. Ionin, L. V. Seleznev, and E. S. Sunchugasheva, Formation of plasma channels in air under filamentation of focused ultrashort laser pulses, Laser Phys. **25**, 033001 (2015).

[4] F. Théberge, N. Aközbek, W. Liu, A. Becker, and S. L. Chin, Tunable Ultrashort Laser Pulses Generated through Filamentation in Gases, Phys. Rev. Lett. **97**, 023904 (2006).

[5] J. Ni, W. Chu, H. Zhang, Ch. Jing, J. Yao, H. Xu, B. Zeng, G. Li, Ch. Zhang, S. L. Chin, Y. Cheng, and Zh. Xu, Harmonic-seeded remote laser emissions in N_2-Ar, N_2-Xe and N_2-Ne mixtures: a comparative study, Opt. Express **20**, 20970 (2012).

[6] H. Sun, J. Liu, Ch. Wang, J. Ju, Zh. Wang, W. Wang, X. Ge, Ch. Li, S. L. Chin, R. Li, and Zh. Xu, Laser filamentation induced air-flow motion in a diffusion cloud chamber, Opt. Express **21**, 9255 (2013).

[7] S. Yuan, T.-J. Wang, H. Pan, L. Zheng, S. L. Chin, and H. Zeng, Pulse polarization evolution and control in the wake of molecular alignment inside a filament, Opt. Express **23**, 5582 (2015).

[8] O. Smirnova and M. Ivanov, Ultrafast science: Towards a one-femtosecond film, Nat. Phys. **6**, 159 (2010).

[9] Yu. E. Geints, A. A. Zemlyanov, N. A. Izyumov, A. A. Ionin, S. I. Kudryashov, L. V. Seleznev, D. V. Sinitsyn, and E. S. Sunchugasheva, Self-focusing of profiled ultrashort-wavelength laser beams in air, Sov. Phys. JETP **116**, 197 (2013).

[10] P. Panagiotopoulos, D. G. Papazoglou, A. Couairon, and S. Tzortzakis, Sharply autofocused ring-Airy beams transforming into non-linear intense light bullets, Nat. Commun. **4**, 2622 (2013).

[11] M. Scheller, M. S. Mills, M.-A. Miri, W. Cheng, J. V. Moloney, M. Kolesik, P. Polynkin, and D. N. Christodoulides, Externally refuelled optical filaments, Nat. Photonics **8**, 297 (2014).

[12] P. Polynkin and M. Kolesik, Critical power for self-focusing in the case of ultrashort laser pulses, Phys. Rev. A **87**, 053829 (2013).

[13] J. P. Palastro, Time-dependent polarization states of high-power, ultrashort laser pulses during atmospheric propagation, Phys. Rev. A **89**, 013804 (2014).

[14] Z. F. Feng, W. Li, C. X. Yu, X. Liu, J. Liu, and L. B. Fu, Extended laser filamentation in air generated by femtosecond annular Gaussian beams, Phys. Rev. A **91**, 033839 (2015).

[15] S. Schiemann, A. Kuhn, S. Steuerwald, and K. Bergmann, Efficient coherent population transfer in NO molecules using pulsed lasers, Phys. Rev. Lett. **71**, 3637 (1993).

[16] I. V. Andrianov and G. K. Paramonov, Selective excitation of the vibrational-rotational states and dissociation of diatomic

molecules by picosecond infrared laser pulses: Modeling for HF in the ground electronic state, Phys. Rev. A **59**, 2134 (1999).
[17] R. Wang, Y.-Y. Niu, M.-H. Qiu, and Y.-Ch. Han, Rovibrational population transfer in the ground state controlled by two coherent laser pulses, Phys. Rev. A **91**, 013401 (2015).
[18] X. M. Tong, Z. X. Zhao, and C. D. Lin, Theory of molecular tunneling ionization, Phys. Rev. A **66**, 033402 (2002).
[19] S.-F. Zhao, C. Jin, A.-T. Le, T. F. Jiang, and C. D. Lin, Determination of structure parameters in strong-field tunneling ionization theory of molecules, Phys. Rev. A **81**, 033423 (2010).
[20] B. A. Zon, Tunneling ionization of atoms with excitation of the core, Sov. Phys. JETP **91**, 899 (2000).
[21] A. S. Kornev and B. A. Zon, Keldysh theory of tunnel ionization of an atom in a few-cycle laser pulse field, Phys. Rev. A **85**, 035402 (2012).
[22] A. S. Kornev and B. A. Zon, Anti-Stokes-enhanced tunneling ionization of polar molecules, Laser Phys. **24**, 115302 (2014).
[23] A. S. Kornev, E. B. Tulenko, and B. A. Zon, Kinetics of multiple ionization of rare-gas atoms in a circularly polarized laser field, Phys. Rev. A **68**, 043414 (2003).
[24] A. S. Kornev, E. B. Tulenko, and B. A. Zon, Ne^+ and Ne^{2+} ion formation in circularly polarized laser fields: Comparison between theory and experiment, Phys. Rev. A **69**, 065401 (2004).
[25] B. A. Zon, A. S. Kornev, and E. B. Tulenko, Many-body effects in the formation of multiply charged ions in a strong laser field, Sov. Phys. JETP **111**, 921 (2010).
[26] A. S. Kornev, E. B. Tulenko, and B. A. Zon, Multiple ionization of Ar, Kr, and Xe in a superstrong laser field, Phys. Rev. A **84**, 053424 (2011).
[27] A. S. Kornev and B. A. Zon, Anti-Stokes-enhanced tunneling ionization of molecules, Phys. Rev. A **86**, 043401 (2012).
[28] A. S. Kornev and B. A. Zon, Relativistic effects in the many-body theory of extreme multiplicity ion formation in superstrong laser fields, Laser Phys. Lett. **10**, 085301 (2013).
[29] A. S. Kornev, I. M. Semiletov, and B. A. Zon, Keldysh theory in a few-cycle laser pulse, inelastic tunneling and Stark shift: Comparison with *ab initio* calculation, J. Phys. B **47**, 204026 (2014).
[30] Y. R. Shen, *The Principles of Nonlinear Optics* (Wiley, New York, 1989).
[31] J. Karczmarek, J. Wright, P. Corkum, and M. Ivanov, Optical Centrifuge for Molecules, Phys. Rev. Lett. **82**, 3420 (1999).
[32] P. A. Bokhan, V. V. Buchanov, N. V. Fateev, M. M. Kalugin, M. A. Kazaryan, A. M. Prokhorov, and D. E. Zakrevskii, *Laser Isotope Separation in Atomic Vapor* (Wiley-VCH, Berlin, 2006).
[33] J. Kobus, A finite difference Hartree–Fock program for atoms and diatomic molecules, Comput. Phys. Commun. **184**, 799 (2013).
[34] A. A. Ratzig and B. M. Smirnov, *Reference Data on Atoms, Molecules and Ions* (Springer, Berlin, 1985).
[35] A. Lofthus and P. H. Krupenie, The spectrum of molecular nitrogen, J. Phys. Chem. Ref. Data **6**, 113 (1977).
[36] L. B. Madsen, F. Jensen, O. I. Tolstikhin, and T. Morishita, Structure factors for tunneling ionization rates of molecules, Phys. Rev. A **87**, 013406 (2013).
[37] Æ. Frisch *et al.*, GAUSSIAN 09, *revision D.01,* Gaussian Inc., Wallingford, CT, 2009.
[38] M. W. Schmidt *et al.*, General atomic and molecular electronic structure system, J. Comput. Chem. **14**, 1347 (1993).
[39] C. Lefebvre, H. Z. Lu, S. Chelkowski, and A. D. Bandrauk, Electron-nuclear dynamics of the one-electron nonlinear polyatomic molecule H_3^{2+} in ultrashort intense laser pulses, Phys. Rev. A **89**, 023403 (2014).
[40] C. R. Mendez, J. R. Vazquez de Aldana, L. Plaja, L. Roso, A. M. Popov, O. V. Tikhonova, P. A. Volkov, and E. A. Volkova, Strong-field short-pulse ionization of the molecular hydrogen ion, Laser Phys. Lett. **1**, 25 (2004).
[41] A. Picón, A. Jaroń-Becker, and A. Becker, Enhancement of Vibrational Excitation and Dissociation of H_{2+} in Infrared Laser Pulses, Phys. Rev. Lett. **109**, 163002 (2012).
[42] M. Fischer, J. Handt, J.-M. Rost, F. Grossmann, and R. Schmidt, Molecular rotation in strong-field ionization, Phys. Rev. A **86**, 053821 (2012).
[43] N. G. Kling, J. McKenna, A. M. Sayler, B. Gaire, M. Zohrabi, U. Ablikim, K. D. Carnes, and I. Ben-Itzhak, Charge asymmetric dissociation of a CO^+ molecular-ion beam induced by strong laser fields, Phys. Rev. A **87**, 013418 (2013).
[44] O. I. Tolstikhin and L. B. Madsen, Retardation Effects and the Born-Oppenheimer Approximation: Theory of Tunneling Ionization of Molecules Revisited, Phys. Rev. Lett. **111**, 153003 (2013).
[45] M. Kotur, C. Zhou, S. Matsika, S. Patchkovskii, M. Spanner, and Th. C. Weinacht, Neutral-Ionic State Correlations in Strong-Field Molecular Ionization, Phys. Rev. Lett. **109**, 203007 (2012).
[46] J. Mikosch, A. E. Boguslavskiy, I. Wilkinson, M. Spanner, S. Patchkovskii, and A. Stolow, Channel- and Angle-Resolved Above Threshold Ionization in the Molecular Frame, Phys. Rev. Lett. **110**, 023004 (2013).
[47] R. Murray, M. Spanner, S. Patchkovskii, and M. Yu. Ivanov, Tunnel Ionization of Molecules and Orbital Imaging, Phys. Rev. Lett. **106**, 173001 (2011).
[48] O. I. Tolstikhin, L. B. Madsen, and T. Morishita, Weak-field asymptotic theory of tunneling ionization in many-electron atomic and molecular systems, Phys. Rev. A **89**, 013421 (2014).
[49] B. A. Zon and B. G. Katsnel'son, Nonresonant scattering of intense light by a molecule, Sov. Phys. JETP **42**, 595 (1975).
[50] B. Friedrich and D. Herschbach, Alignment and Trapping of Molecules in Intense Laser Fields, Phys. Rev. Lett. **74**, 4623 (1995).
[51] B. A. Zon, Classical theory of the molecule alignment in a laser field, Eur. Phys. J. D **8**, 377 (2000).
[52] I. S. Averbukh and R. Arvieu, Angular Focusing, Squeezing, and Rainbow Formation in a Strongly Driven Quantum Rotor, Phys. Rev. Lett. **87**, 163601 (2001).
[53] H. Stapelfeldt and T. Seideman, Colloquium: Aligning molecules with strong laser pulses, Rev. Mod. Phys. **75**, 543 (2003).
[54] I. V. Litvinyuk, K. F. Lee, P. W. Dooley, D. M. Rayner, D. M. Villeneuve, and P. B. Corkum, Alignment-Dependent Strong Field Ionization of Molecules, Phys. Rev. Lett. **90**, 233003 (2003).
[55] B. A. Zon, Born-Oppenheimer approximation for molecules in a strong light field, Chem. Phys. Lett. **262**, 744 (1996).
[56] K. Aidas *et al.*, The Dalton quantum chemistry program system, WIREs Comput. Mol. Sci. **4**, 269 (2014).
[57] DALTON, a molecular electronic structure program, release Dalton2015.0, 2015, http://daltonprogram.org.